
Research article

Foldable structures made of hydrogel bilayers

Virginia Agostiniani¹, Antonio DeSimone^{2,*}, Alessandro Lucantonio² and Danka Lučić²

¹ Computer Science Department, University of Verona, Strada le Grazie 15, 37134 Verona - Italy

² SISSA - International School for Advanced Studies, via Bonomea 265, 34136 Trieste - Italy

* Correspondence: Email: desimone@sissa.it.

Abstract: We discuss self-folding of a thin sheet by using patterned hydrogel bilayers, which act as hinges connecting flat faces. Folding is actuated by heterogeneous swelling due to different cross-linking densities of the polymer network in the two layers. Our analysis is based on a dimensionally reduced plate model, obtained by applying a recently developed theory [1], which provides us with an explicit connection between (three-dimensional) material properties and the curvatures induced at the hinges. This connection offers a recipe for the fabrication and design of the bilayers, by providing the values of the cross-linking density of each layer that need to be imprinted during polymerization in order to produce a desired folded shape upon swelling.

Keywords: hydrogels; folding; bilayers; dimension reduction; Gamma-convergence; Kirchhoff plate theory

1. Introduction

The study of shape programming and morphing of surfaces is receiving considerable attention, especially in the field of active (or *smart*) materials, i.e. materials that deform in response to non-mechanical stimuli. Of particular interest is the problem of exploiting material heterogeneities to induce complex shape changes—for instance, to produce curved configurations from an initially flat state [2–6]. In many natural systems, such as plants [7, 8], shape control is usually accomplished by growth, remodelling, or swelling, in response to simple external stimuli (e.g. a uniform change in the ambient temperature or humidity). To mimic such behaviors, synthetic soft active materials appear as suitable candidates. Hydrogels are examples of active materials where spontaneous deformations are induced by swelling due to the absorption of a liquid. In the form of bilayers, they can be employed to produce curved shapes [9].

Self-folding is a widespread phenomenon that occurs in natural systems, such as in the opening and closing of flowers. The understanding of such mechanisms offers interesting challenges and

opportunities, not only from the point of view of biology, but also from the point of view of applications, for instance, in the fabrication of actuation systems and origami-like structures [10]. Self-folding results from spatially heterogeneous deformations that are (in most cases) either induced by a spatial variation of the external stimulus or by modulations of the material properties imprinted during the fabrication process. We refer to [11–16] for some examples of the approaches to folding and the numerical models that might be used in the study of folding mechanisms.

In this paper, we discuss self-folding of thin sheets by using hydrogel bilayers, which act as hinges connecting flat faces. Folding is actuated by the heterogeneous swelling due to different stiffness (i.e. cross-linking density) of the polymer network across two layers. More precisely, we will focus on the case where the cross-linking density in the top and the bottom layers is a perturbation (of magnitude comparable to the total thickness of the plate, which is a small parameter) of an average constant density \bar{N} , see formula (2.1). We show that this structure allows to endow a thin gel sheet with a controlled curvature localized at the hinges (see Figure 1), which can be realized upon swelling at low energy cost. Furthermore, such a curvature can be expressed as a function of the material parameters of the layers. Specifically, we demonstrate the feasibility of the proposed folding mechanism with two examples, corresponding to specific patterns of flat faces and hinges (see Figure 2).

Our approach to the analysis of hydrogel-based folding sheets exploits the two-dimensional (nonlinear) plate model presented in Subsection 2.1, which is obtained by applying the rigorously derived theory [1] for heterogeneous thin elastic plates based on Γ -convergence arguments. The value of employing such a rigorously derived theory is twofold: first, we avoid inconsistencies often present in *ad hoc*, formally-deduced models by performing a mathematically rigorous limit; second, the material and geometric parameters of the reduced 2D model emerge from (i.e. are computed from) those of the 3D one, which are the only ones that are accessible from the point of view of the sample preparation in a laboratory, hence ensuring that the minimizers of the 2D model faithfully reproduce the true behavior of sufficiently thin (yet, three-dimensional) bilayers. In Section 3 we study the pointwise energy minimizers of the plate model, which describe the configurations of a plate with bilayer-like hinges and thus provide a theoretical justification for the effectiveness of the folding mechanism. In Section 4, with reference to an appropriate approximate variant of our Flory-Rehner-type model, we provide the explicit relation between the target curvature and the material parameters, see (4.25). Such relation is then used in the design of folding bilayer sheets that morph into cubes or pyramids. We end the paper with an appendix, where we provide a detailed analysis of Flory-Rehner-type energy densities and show how the dimension-reduction framework studied in [1] applies to the model considered here.

2. Self-folding using bilayer gels

Let us call $\Omega_{h_0} = \omega \times (-h_0/2, h_0/2)$ the reference configuration of our foldable structure, where the reference thickness h_0 is much smaller than the in-plane dimensions. The planar domain ω , which represents the mid-plane of the plate, is hereafter assumed to be a union $\omega = \bigcup_{i=1}^n \omega_i$ of polygons. We denote by $x = (x_1, x_2, x_3) = (x', x_3)$ an arbitrary point in Ω_{h_0} . We say that the interfaces which delimit the polygons form a *pattern* on ω .

To model our system, we consider a family $\{W_h\}$ of 3D free-energy densities, from which we can derive the corresponding 2D Kirchhoff bending model (i.e. the energies scale as h^3) in the vanishing

thickness limit, by using the rigorous derivation recently provided in [1]. At the same time, W_{h_0} represents the actual energy density corresponding to the finite (small) thickness system. A thin sheet with ideal small thickness h is supposed to be a heterogeneous system where the heterogeneity, both lateral and vertical, is due to a patterned bilayer structure made of hydrogels. This structure is engineered through an x -dependent density of cross-links in the polymer network, which in turn determines an x -dependent density $N_h(x)$ of polymer chains. More precisely, we suppose that

$$N_h(x) = \begin{cases} \bar{N} - \frac{h}{h_0} M_i, & \text{for } x \in \omega_i \times (-h/2, 0], \\ \bar{N} + \frac{h}{h_0} M_i, & \text{for } x \in \omega_i \times (0, h/2), \end{cases} \quad (2.1)$$

for some constants $\bar{N} > 0$ and $M_i \geq 0$, $i = 1, \dots, n$. Note that the average density along the thickness $\int_{-1/2}^{1/2} N_h(x', x_3) dx_3$ is supposed to be constant in x' and equal to \bar{N} .

The system is a composite of flat faces (where $M_i = 0$) connected by hinges (where $M_i > 0$). Starting from an initially dry state, folding will be accomplished by putting the gel in contact with a solvent. Upon swelling, the difference in N_h in the two layers of the hinges will induce bending. The prototype of this actuation mechanism is presented in Figure 1, where the larger (resp. lower) number of dots in the hinge (red patch) corresponds to a higher (resp. lower) cross-linking density in each layer.

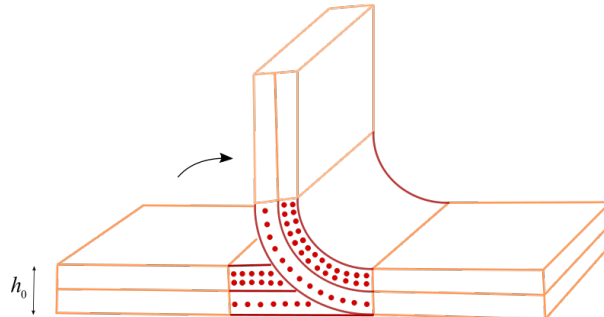


Figure 1. Sketch of the proposed folding mechanism. The hydrogel bilayer acts as a hinge that bends upon swelling. The number of red dots in each of the two layers is proportional to the amount of cross-links in the polymer network.

For the constitutive model of the hydrogel, we use an energy density of Flory-Rehner type [17], which takes into account both the elastic and the mixing energy contributions. Namely,

$$W_h(x, F) := \frac{vN_h(x)}{2}(|F|^2 - 3) + W_{vol}^\chi(\det F) - \frac{\mu}{kT}(\det F - 1), \quad (2.2)$$

where $x \in \Omega_h$ and F , which represents a deformation gradient, belongs to the class $\mathbb{R}_1^{3 \times 3}$ of all the 3×3 matrices with $\det F \geq 1$. The last term in the above expression is the energy of the solvent within the gel, whereas the mixing energy W_{vol}^χ is defined in $(1, +\infty)$ by

$$W_{vol}^\chi(t) := (1-t) \log\left(\frac{t}{t-1}\right) - \frac{\chi}{t} + \chi. \quad (2.3)$$

Moreover, the parameters appearing in (2.2) are:

- k - Boltzmann's constant;
- T - absolute temperature of the environment;
- v - volume per solvent molecule;
- $\chi \in (0, 1/2]$ - dimensionless measure of the enthalpy of mixing;
- $\mu \leq 0$ - chemical potential of the solvent molecules within the gel.

Note that the range $\mu \leq 0$ corresponds to having a gel in contact with an external fluid that is either a vapor ($\mu < 0$) or a pure liquid in equilibrium with its own vapor ($\mu = 0$). Finally, the range $\chi \in (0, 1/2]$, which corresponds to a “good” solvent, implies in particular that W_{vol}^χ is a strictly decreasing function fulfilling

$$\lim_{t \rightarrow 1^+} W_{vol}^\chi(t) = 0 \quad \text{and} \quad \lim_{t \rightarrow +\infty} W_{vol}^\chi(t) = \chi - 1 < 0.$$

As a consequence of the heterogeneity of W_h , which is due to the heterogeneous density of polymer chains N_h , the energy well will in turn be x -dependent. More precisely, from the computations in Appendix A (see (A.35) and (A.38)–(A.39)) we have that there exist two constants

$$\alpha > 1 \quad \text{and} \quad \beta \neq 0, \tag{2.4}$$

which depend on k , on the (fixed) material parameters of the gel v, χ , and average density N , and on the environmental conditions (μ, T) , such that

$$\operatorname{argmin}_{\mathbb{R}_1^{3 \times 3}} W_h(x, \cdot) = U_h(x) \operatorname{SO}(3), \tag{2.5}$$

where, for every $x \in \Omega_h$, $U_h(x)$ is the scalar multiple of the identity matrix given by

$$U_h(x) := \begin{cases} \alpha I_3 - \frac{h}{h_0} \beta M_i I_3 + o(h), & \text{if } x \in \omega_i \times (-h/2, 0], \\ \alpha I_3 + \frac{h}{h_0} \beta M_i I_3 + o(h), & \text{if } x \in \omega_i \times (0, h/2). \end{cases} \tag{2.6}$$

The map $x \mapsto U_h(x)$ is the *spontaneous stretch* field that characterizes the *relaxed* (zero-stress) state the system would try to attain spontaneously, at each point x , through a deformation with gradient $U_h(x)$. The two constant matrices αI_3 and $\frac{h}{h_0} \beta M_i I_3$ have been written separately in definition (2.6) to stress their different contributions as stretching and bending terms, respectively (see equations (2.8)–(2.9) defining the reduced model, where α enters the definition of the class on which such model is constrained and β in that of the target curvature).

For every $0 < h \ll 1$, the *total energy* of the system associated with a deformation $v_h \in W^{1,2}(\Omega_h, \mathbb{R}^3)$ in the absence of external loads is given by the quantity

$$\mathcal{E}_h(v_h) := \int_{\Omega_h} W_h(x, \nabla v_h(x)) dx. \tag{2.7}$$

The choice of the functional space $W^{1,2}(\Omega_h, \mathbb{R}^3)$ is natural since a finite energy $\mathcal{E}_h(v_h)$ implies that $v_h \in W^{1,2}(\Omega, \mathbb{R}^3)$ (see the lower bound (A.49) in Appendix A).

2.1. Two-dimensional model of a thin gel sheet

The 3D model presented in Section 2 falls within the general framework studied in [1] for the derivation of the corresponding 2D Kirchhoff model, via Γ -convergence arguments. This is proved explicitly in Appendix A. A direct consequence of this fact is that any low-energy sequence $\{v_h\}_h$ of the scaled 3D energies $\frac{1}{h^3}\mathcal{E}_h$ converges (in the $W^{1,2}$ topology) to a deformation y that minimizes the 2D energy defined, up to constant terms, as

$$\mathcal{E}_0(u) := \frac{1}{24} \int_{\omega} \mathbb{C}(A_u(x') - \bar{A}(x')) \cdot (A_u(x') - \bar{A}(x')) dx', \quad u \in W_{\alpha,\text{iso}}^{2,2}(\omega), \quad (2.8)$$

on the class $W_{\alpha,\text{iso}}^{2,2}(\omega)$ of all $u \in W^{2,2}(\omega, \mathbb{R}^3)$ such that $(\nabla u)^T \nabla u = \alpha^2 I_2$. We recall that, up to an α -dilation, any $u \in W_{\alpha,\text{iso}}^{2,2}(\omega)$ is a C^1 -isometric immersion of ω into \mathbb{R}^3 , which admits jumps of curvature.

In formula (2.8), A_u is the second fundamental form associated with u and expressed in terms of the “undeformed” in-plane variable x' . Namely, with the following choice $v(x')$ of the unit normal to the surface $u(\omega)$ at $u(x')$,

$$A_u(x') := (\nabla u(x'))^T \nabla v(x'), \quad v(x') := \frac{\partial_1 u(x') \wedge \partial_2 u(x')}{|\partial_1 u(x') \wedge \partial_2 u(x')|},$$

The *target curvature* tensor \bar{A} is a piecewise constant map, which is defined on each subdomain ω_i of ω by

$$\bar{A} = \bar{a}_i I_2, \quad \text{with} \quad \bar{a}_i := \frac{3\beta}{h_0} M_i, \quad i = 1, \dots, n. \quad (2.9)$$

Moreover, the fourth-order tensor \mathbb{C} is given by

$$\mathbb{C} := 2G I_2 + \Lambda(\alpha) I_2 \otimes I_2, \quad (2.10)$$

where G and $\Lambda(\alpha)$ are non-dimensional positive Lamé constants, which can be expressed in terms of the material parameters as

$$G := v\bar{N} \quad \text{and} \quad \Lambda(\alpha) := \frac{2G\lambda(\alpha)}{2G + \lambda(\alpha)} > 0, \quad \text{with} \quad \lambda(\alpha) := \left(-v\bar{N} - \frac{1}{\alpha^2} + \frac{\alpha}{\alpha^3 - 1} - \frac{2\chi}{\alpha^5} \right) > 0. \quad (2.11)$$

The positivity of $\lambda(\alpha)$ is not self evident from the above formula and due to the fact that α depends in particular on v , \bar{N} , and χ (see formulas (A.35) and (A.47)–(A.48) with $\theta = 1$ in Appendix A).

Another direct consequence of the Γ -convergence result mentioned at the beginning of this subsection, which we now emphasize in terms of the physical quantities and the finite thickness h_0 (small with respect to the in-plane characteristic size of the plate), the following asymptotic approximate identity for the low-energy values $\mathcal{E}_{h_0}(v_{h_0}) = \inf \mathcal{E}_{h_0} + o(1)$:

$$\mathcal{E}_{h_0}(v_{h_0}) \cong \frac{h_0^3}{24} \int_{\omega} \mathbb{C}(A_y(x') - \bar{A}(x')) \cdot (A_y(x') - \bar{A}(x')) dx' + \text{ad.t..} \quad (2.12)$$

Here, the additional term “ad.t.” is given by the formula

$$\text{ad.t.} = \frac{h_0 \beta^2 (G + \Lambda(\alpha))}{2} \left(\sum_{i=1}^n M_i^2 |\omega_i| \right). \quad (2.13)$$

Hence, the minimizers of the 2D bending model (2.8) provide reliable estimates for the “almost minimal” values of the 3D energy given by (2.2) and (2.7). Also, the positivity of the additional term (due to (2.11)) tells us that the 2D energy cannot be minimized at the value zero: this fact originates in the incompatibility of the spontaneous strain distribution and hence in the presence of residual stresses in the 3D reference configuration.

3. Minimal energy configurations: connection between shape parameters and gel properties

In this section, we study the minimizers of the limiting bending energy \mathcal{E}_0 given by (2.8). More precisely, we focus our attention on the class of *pointwise minimizers*, namely, on those deformations $y \in W_{\alpha,\text{iso}}^{2,2}(\omega)$ whose second fundamental form A_y minimizes pointwise the integrand in (2.8). Importantly, this analysis employs a simple structure from the fabrication viewpoint and provides the theoretical basis for successful and robust actuation using the proposed folding mechanism.

Let us first operate an affine change of variable by associating to each $y \in W_{\alpha,\text{iso}}^{2,2}(\omega)$ a corresponding isometry $\tilde{y} \in W_{1,\text{iso}}^{2,2}(\alpha\omega)$, via

$$\tilde{y}(\eta') := y\left(\frac{\eta'}{\alpha}\right), \quad \eta' \in \alpha\omega. \quad (3.14)$$

The second fundamental forms associated with y and \tilde{y} are related via the formula

$$A_{\tilde{y}}(\eta') = \frac{1}{\alpha^2} A_y\left(\frac{\eta'}{\alpha}\right), \quad \eta' \in \alpha\omega. \quad (3.15)$$

In turn, we get that

$$\begin{aligned} \min_{y \in W_{\alpha,\text{iso}}^{2,2}(\omega)} \int_{\omega} \mathbb{C}(A_y(x') - \bar{A}(x')) \cdot (A_y(x') - \bar{A}(x')) dx' \\ = \min_{\tilde{y} \in W_{1,\text{iso}}^{2,2}(\alpha\omega)} \frac{1}{\alpha^2} \int_{\alpha\omega} \mathbb{C}(\alpha^2 A_{\tilde{y}}(\eta') - \bar{A}(\eta'/\alpha)) \cdot (\alpha^2 A_{\tilde{y}}(\eta') - \bar{A}(\eta'/\alpha)) d\eta'. \end{aligned} \quad (3.16)$$

According to (2.9) and (3.16), and recalling that each isometry \tilde{y} is such that $\det A_{\tilde{y}} = 0$ a.e. in $\alpha\omega$, our minimization problem reduces to finding those isometries \tilde{y} whose second fundamental form fulfills

$$A_{\tilde{y}}(\eta') \in \mathcal{N}_i := \operatorname{argmin}_{\substack{A \in \text{Sym}(2) \\ \det A = 0}} \mathbb{C}(a^2 A - \bar{a}_i I_2) \cdot (a^2 A - \bar{a}_i I_2), \quad \text{for a.e. } \eta' \text{ in the } i\text{-th subdomain of } \alpha\omega, \quad (3.17)$$

for every $i = 1, \dots, n$, where \bar{a}_i is defined as in (2.9). A necessary and sufficient condition for (3.17) to hold is that $A_{\tilde{y}}$ is actually equal to a constant $A_i \in \mathcal{N}_i$ on each i -th subdomain of $\alpha\omega$ (for the necessity of such condition we refer the reader to [18]).

The solution of the (finite dimensional) minimization problem in (3.17), as done in [1, Lemma 3.1], yields the following explicit representation for the set \mathcal{N}_i :

$$\mathcal{N}_i = \left\{ \frac{\kappa_i}{\alpha^2} \mathbf{n} \otimes \mathbf{n} : \mathbf{n} \in \mathbb{R}^2, \text{ with } |\mathbf{n}| = 1 \right\}, \quad \text{with } \kappa_i := 2 \bar{a}_i \frac{G + \Lambda(\alpha)}{2G + \Lambda(\alpha)}, \quad i = 1, \dots, n. \quad (3.18)$$

In other words, the second fundamental form $A_{\tilde{y}}$ of an energy minimizing isometry \tilde{y} , when restricted to the i -th subdomain of $\alpha\omega$ (that we refer to as the i -th patch) with $\kappa_i \neq 0$, corresponds to the second

fundamental form of a *cylindrical surface* whose non-zero principal curvature equals κ_i/α^2 , while the associated principal curvature direction might be (*a priori*) given by any unit vector in \mathbb{R}^2 . However, the isometry constraint forces a precise choice of the principal curvature direction associated with the non-zero principal curvature κ_i/α^2 – it must be orthogonal to the interfaces between i -th patch and all the neighboring ones. Equivalently, a cylindrical surface with $\kappa_i \neq 0$ can be glued to all the neighboring cylindrical surface patches (or even plane patches) only if its rulings are parallel to the interface between them. It is thus clear that the existence of an isometry with the above described properties heavily depends on the compatibility between the pattern on ω and the target curvature, as proved in [1, Theorem 3.9].

The theoretical results that we have just discussed provide the foundations for a successful self-folding strategy in patterned, bilayer thin sheets made of hydrogels (or other active materials). In particular, the planar domain ω is patterned in such a way that the heterogeneity in swelling of the gel due to variations in the cross-linking density induces piecewise constant target curvatures. Many interesting and feasible patterns on ω along with the induced target curvatures at the hinges satisfy the previously mentioned compatibility property, thus guaranteeing the existence of a pointwise minimizer of the 2D bending energy. To be concrete, we now consider the *pyramid-type* and the *cube-type* domains, sketched in the Figure 2 (A) and (B), respectively. Both of these two patterned domains consist of two different types of patches: *hinges* and *flat faces*.

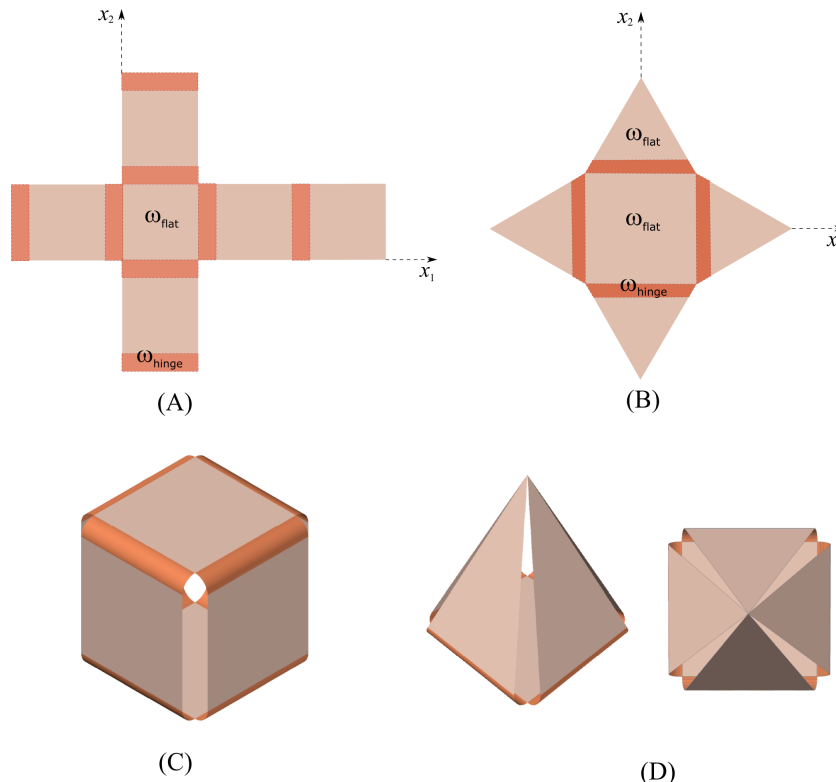


Figure 2. Cube-type domain (A) and pyramid-type domain (B) in the unfolded flat state. Folded cube shape (C) and pyramid shape (D) obtained as images of the corresponding patterned domains (A) and (B) under the pointwise minimizing deformation of the corresponding 2D bending energies.

Each hinge, denoted by ω_{hinge} , has a nontrivial bilayer structure, characterized by

$$N_h(x) = \begin{cases} \bar{N} - \frac{h}{h_0}M, & \text{for } x \in \omega_{\text{hinge}} \times (-h/2, 0], \\ \bar{N} + \frac{h}{h_0}M, & \text{for } x \in \omega_{\text{hinge}} \times (0, h/2), \end{cases} \quad (3.19)$$

with $M > 0$. On each flat face, denoted by ω_{flat} , the density of polymer chains N_h is constantly equal to \bar{N} , i.e. $M = 0$. Note that both in the pyramid and the cube case the interfaces between an ω_{hinge} and the (at most two) neighboring ω_{flat} are mutually parallel (recall that the set of the nonzero principal curvature directions of a pointwise minimizer restricted to ω_{hinge} may be any unit vector of \mathbb{R}^2 , see (3.18)). Hence the existence of a pointwise minimizer of \mathcal{E}_0 is guaranteed. More in detail, such minimizer deforms the mid-plane ω in the following way: it dilates the domain ω by the factor α and maps each α -dilated hinge into a cylindrical surface with radius $r = \alpha^2/|\kappa|$, where

$$\kappa = \frac{6\beta M}{h_0} \frac{v\bar{N} + \Lambda(\alpha)}{2v\bar{N} + \Lambda(\alpha)}; \quad (3.20)$$

the cylinder's rulings are parallel to the interfaces which delimit the hinge from the flat faces. At the same time, each α -dilated flat face remains flat.

Looking at the expression (3.20) for the curvature κ that arises on the hinges, it is clear that, maintaining the other physical constants fixed, an appropriate choice of the values \bar{N} and M of the bilayer structure at the hinges (recall that $\Lambda(\alpha)$ is \bar{N} -dependent as well, see formula (2.11) and the subsequent paragraph) is needed to induce precise self-folding as in Figure 2 (C) and (D). We address the problem of designing the structure of each bilayer to produce the desired shape upon folding in the following section.

4. Bilayer design problem

In this section we address the “inverse” problem of finding the physical properties of a hydrogel that allow us to realize a given target shape upon self-folding. First, we introduce an approximate variant of the Flory-Rehner energies W_h , for which the dependence of the target curvature \bar{A} on the fixed physical parameters of the 3D system becomes explicit. Further, we restrict our attention to gels characterized by

- $\mu = 0$
- v, \bar{N} and χ satisfying the relation $\bar{N} < \frac{1-2\chi}{2v}$.

The first of these two conditions means that the gel is in contact with a pure liquid in equilibrium with its own vapor. The second condition is always satisfied whenever a hydrogel with a large swelling ratio is considered, as it occurs for the typical values $\bar{N}v \sim 10^{-3}$ and $\chi \sim 10^{-1}$.

To present the approximate model we work with, let us go back to the general setting of a thin gel sheet occupying the domain $\Omega_h = \omega \times (-h/2, h/2)$, with $\omega = \bigcup_{i=1}^n \omega_i$ being a general patchwork of polygons. First of all, in the case $\mu = 0$ the Flory-Rehner energy density (2.2) reduces to

$$W_h(x, F) = \frac{vN_h(x)}{2}(|F|^2 - 3) + W_{vol}^\chi(\det F), \quad (x, F) \in \Omega_h \times \mathbb{R}_1^{3 \times 3}.$$

Then, by Taylor's expansion, $W_{vol}^\chi(t) = \frac{1-2\chi}{2t} + o\left(\frac{1}{t}\right) + \chi - 1$, for every $t \gg 1$. Thus, when deformation gradients with large determinants are considered, one may approximate W_h (discarding the constant term $\chi - 1$) by

$$\widehat{W}_h(x, F) := \frac{vN_h(x)}{2}(|F|^2 - 3) + \frac{1-2\chi}{2 \det F}, \quad (x, F) \in \Omega_h \times \mathbb{R}_1^{3 \times 3}. \quad (4.21)$$

This approximate model is adequate from the point of view of applications. It has been considered for the first time in [17], and afterward used, for instance, in [19, 20].

The functional form (4.21) for the energy densities \widehat{W}_h allows us to determine the associated spontaneous stretch distribution explicitly in terms of the fixed physical parameters of the model. Indeed, from Remark 1 in Appendix A, for every $x \in \omega_i \times (-h/2, h/2)$, $i = 1, \dots, n$, we have

$$\operatorname{argmin}_{\mathbb{R}_1^{3 \times 3}} \widehat{W}_h(x, \cdot) = \widehat{U}_h(x) \operatorname{SO}(3), \quad (4.22)$$

where, for every $x \in \Omega_h$, $\widehat{U}_h(x)$ is the scalar multiple of the identity matrix given by

$$\widehat{U}_h(x) = \begin{cases} \alpha I_3 - \frac{h}{h_0} \beta M_i I_3 + o(h), & \text{if } x \in \omega_i \times (-h/2, 0], \\ \alpha I_3 + \frac{h}{h_0} \beta M_i I_3 + o(h), & \text{if } x \in \omega_i \times (0, h/2), \end{cases} \quad (4.23)$$

and the constants α and β are explicitly given by

$$\alpha = \left(\frac{1-2\chi}{2vN} \right)^{1/5} \quad \text{and} \quad \beta = -\frac{1}{5N} \left(\frac{1-2\chi}{2vN} \right)^{1/5}. \quad (4.24)$$

In this case, the constant $\Lambda(\alpha)$ appearing in (2.11) can be explicitly derived, as well. Thus, by Remark 3 (in particular, formula (A.53)) in Appendix A we obtain that the tensor \mathbb{C} in (2.8), within this approximate 2D model, reads

$$\mathbb{C} = 2v\bar{N} \left(\mathbb{I}_2 + \frac{1}{3} \mathbb{I}_2 \otimes \mathbb{I}_2 \right).$$

Finally, as a consequence of (4.24), the target curvature \bar{A} is given on each subdomain ω_i of ω by

$$\bar{A} = \bar{a}_i \mathbb{I}_2, \quad \text{with} \quad \bar{a}_i := -\frac{3}{5\bar{N}} \left(\frac{1-2\chi}{2v\bar{N}} \right)^{1/5} \frac{M_i}{h_0}, \quad i = 1, \dots, n. \quad (4.25)$$

Summarizing, the total energy (2.8) in this case is

$$\mathcal{E}_0(u) = \frac{v\bar{N}}{12} \sum_{i=1}^n \int_{\omega_i} |\mathbf{A}_u(x') - \bar{a}_i \mathbb{I}_2|^2 + \frac{1}{3} \operatorname{tr}^2(\mathbf{A}_u(x') - \bar{a}_i \mathbb{I}_2) dx', \quad (4.26)$$

for every $u \in W_{\alpha, \text{iso}}^{2,2}(\omega)$. In particular, whenever a compatible pattern is considered, from the discussion at the end of Section 3 and from formula (3.18), it follows that the isometry $\tilde{\gamma}$ associated with a pointwise minimizer y of \mathcal{E}_0 via (3.14), maps each i -th subdomain of $\alpha\omega$ into a cylindrical surface of radius

$$r_i := \frac{4\alpha^2 h_0}{3vM_i} \left(\frac{1-2\chi}{2v\bar{N}} \right)^{-1/5}, \quad (4.27)$$

and with rulings parallel to the interface with each neighboring patch.

We are now ready to design a bilayer structure on each ω_{hinge} (i.e. to determine the values of \bar{N} and M on such subdomain, see (3.19)), in order to induce precise self-folding of a pyramid and a cube (Figure 2 (C) and (D)), at the minimum energy cost.

Pyramid The target shape that we refer to as a (precisely) *folded pyramid* is characterized by the following set of parameters (see Figure 3):

- ℓ – initial length of the pyramid basis,
- $\phi \in (0, \pi/2)$ – vertex angle,
- H – height of the pyramid,
- $\alpha > 1$ – in-plane swelling factor.

By ‘precisely folded pyramid’ we mean that the four external vertices of the unfolded pyramid meet at a single point in the folded configuration. The above four parameters completely determine a (unique) ‘precisely folded pyramid’ shape, since from then one can derive

- r – radius of curvature of the deformed (α -dilated) hinges,
- ℓ_1 – initial hinge width,
- ℓ_2 – initial height of the pyramid side,

via the formulas

$$r = \frac{\sin \phi}{1 + \sin \phi} \left(H - \frac{\alpha \ell}{2 \tan \phi} \right), \quad \ell_1 = \frac{r}{\alpha} \left(\frac{\pi}{2} + \phi \right), \quad \ell_2 = \frac{H - r(1 + \sin \phi)}{\alpha \cos \phi}.$$

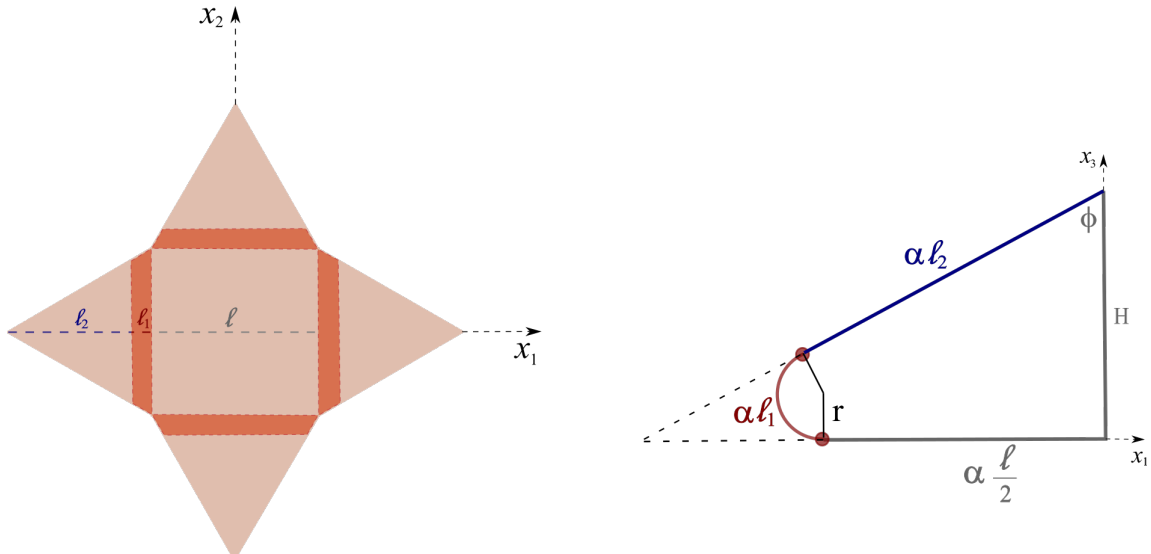


Figure 3. Unfolded pyramid (left) and geometry of the precisely folded pyramid (right).

By using the first formula in (4.24) and expression (4.27), we deduce that the correct material properties (\bar{N} and M) to be imprinted on the hinges in order to accomplish the desired self-folding are

determined in terms of the swelling factor α and the curvature radius r by

$$\bar{N} = \frac{1 - 2\chi}{2v\alpha^5} \quad \text{and} \quad M = \frac{4\alpha^3 h_0}{3vr}. \quad (4.28)$$

Cube We consider as the target shape the (precisely) *folded cube* characterized by the following parameters (see Figure 4):

- ℓ_1 – initial width of the hinge
- $\alpha > 1$ – swelling factor
- $\phi = \pi/2$ – hinge closing angle

The radius r of a cylindrical surface representing a deformed hinge, which is needed to obtain the desired folded cube from a flat, cube-type pattern, must satisfy the relation $r = \frac{2\alpha\ell_1}{\pi}$. As in the pyramid case, formulas (4.24) and (4.27) allow us to design the hinges in order to get a (precisely) folded cube. Namely, the material parameters that determine the cross-linking density in the bilayers that constitute the hinges are

$$\bar{N} = \frac{1 - 2\chi}{2v\alpha^5} \quad \text{and} \quad M = \frac{4\alpha^3 h_0}{3vr} = \frac{2\alpha^2 \pi h_0}{3v\ell_1}. \quad (4.29)$$

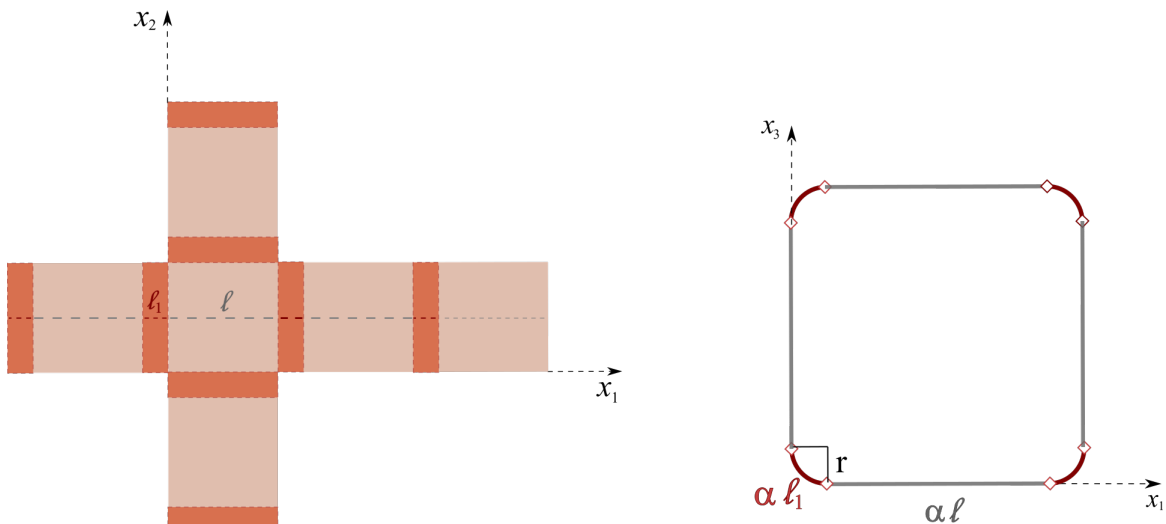


Figure 4. Unfolded cube on the left, geometry of the precisely folded cube on the right.

As it is clear from the above formulas, the final ‘size’ of a folded cube or pyramid is controlled by the parameter \bar{N} through its relation with the swelling factor α . Specifically, in order to produce larger folded cubes or pyramids, which correspond to a bigger value of α , a smaller value of \bar{N} is needed. The curvature of the hinges $1/r$ is controlled by the parameter M , in such a way that, as one might expect, the value of r increases as the value of M decreases. This means that, on one side, flat plates (seen as cylindrical surfaces with radius $r = +\infty$) correspond to the isometric deformation of patches with no through-the-thickness variation of the cross linking density, i.e. $M = 0$. On the other side, shapes with sharp folds (i.e. with $r \rightarrow 0$) require large variations M in the cross-linking density along the bilayer that constitutes the hinge. In turn, since r and ℓ_1 are proportional, manufacturing a folded structure with a small hinge width ℓ_1 requires a large value of M .

5. Conclusion

We have shown how patterned, thin hydrogel bilayers can be employed to realize self-folding structures. Specifically, folding can be achieved upon swelling by inserting hydrogel bilayers with varying cross-linking density across the thickness as hinges between flat faces, where the material is homogeneous.

Using rigorous dimension reduction techniques, we have obtained a two-dimensional plate model that describes the mechanics of such a system. Then, the study of the pointwise minimizers of the 2D model has suggested a successful strategy for the realization of foldable structures with programmable shape. In particular, folded structures arise as pointwise minimizers of the 2D energy whenever the pattern of hinges and flat faces satisfy the compatibility conditions determined in [1]. These conditions provide the theoretical basis for successful and robust actuation.

A major result of the dimension reduction procedure is to provide us with the connection between material properties (a feature of the 3D model) and the induced curvature upon swelling (a feature of the 2D model). We have then exploited such a connection as a tool for the design of the bilayer structure able to produce target folded shapes (specifically, cubes and pyramids).

The richness of emergent shapes found in nature that one would like to mimic using synthetic systems is, of course, not limited to configurations obtainable as pointwise minimizers. This strongly motivates further, more general, studies of the geometry of the minimal energy configurations of the 2D bending functional (2.8), as well as the derivation of new dimensionally reduced models allowing, for instance, for the presence of both bending and stretching contributions in the 2D energy.

A. Appendix

This section is devoted to the analysis of the Flory-Rehner-type energy density functions W_h introduced in (2.2). Letting all the physical parameters (ν, χ, μ, k and T) be fixed and letting the mid-plane of the plate ω be a union of polygons ω_i , we recall that

$$W_h(x, F) := \frac{\nu N_h(x)}{2}(|F|^2 - 3) + W_{vol}^\chi(\det F) - \frac{\mu}{kT}(\det F - 1), \quad (x, F) \in \Omega_h \times \mathbb{R}_+^{3 \times 3}, \quad (\text{A.30})$$

for every small thickness parameter $0 < h \ll 1$. We refer to (2.3) for the definition of W_{vol}^χ . For later use it is convenient to introduce the following equivalent normalized expression for the density of polymer chains:

$$N_h(x) = \bar{N} f_h(x), \quad \text{where} \quad f_h(x) := \begin{cases} 1 - \frac{h}{h_0} \frac{M_i}{\bar{N}}, & \text{for } x \in \omega_i \times (-h/2, 0], \\ 1 + \frac{h}{h_0} \frac{M_i}{\bar{N}}, & \text{for } x \in \omega_i \times (0, h/2). \end{cases} \quad (\text{A.31})$$

Note that for every $F \in \mathbb{R}_+^{3 \times 3} := \{F \in \mathbb{R}^{3 \times 3} : \det F > 0\}$, by a standard algebraic inequality we have that

$$|F|^2 = \lambda_1^2 + \lambda_2^2 + \lambda_3^2 \geq 3(\lambda_1^2 \lambda_2^2 \lambda_3^2)^{1/3} = 3(\det(F^T F))^{1/3} = 3(\det F)^{2/3}, \quad (\text{A.32})$$

where $\lambda_1^2, \lambda_2^2, \lambda_3^2$ are the eigenvalues of the matrix $F^T F$, and where the equality holds if and only if $\lambda_1^2 = \lambda_2^2 = \lambda_3^2$. In particular, we have that

$$W_h(x, F) \geq p(f_h(x), \det F),$$

where $p : (0, +\infty) \times [1, +\infty) \rightarrow \mathbb{R}$ is defined as

$$p(\theta, t) := \frac{3v\bar{N}}{2}\theta(t^{2/3} - 1) + W_{vol}^\chi(t) - \frac{\mu}{kT}(t - 1). \quad (\text{A.33})$$

The above inequality, and the related rigidity characterizing the equality case, says in particular that F_{\min} is a minimizer of $W_h(x, \cdot)$ if and only if $F_{\min} = t_{\min}^{1/3}R$, for some $R \in \text{SO}(3)$, where t_{\min} is a minimizer of $p(f_h(x), \cdot)$. This argument is detailed in the proof of Lemma 3 below.

In view of the previous discussion and since $f_h(x)$ is uniformly close to 1 for every h sufficiently small, in what follows we analyze the minimizers of $p(\theta, \cdot)$, for θ varying in some interval \mathcal{I} containing 1. To do this, it is useful to recall the following sharp logarithmic estimate (which can be found in [21])

$$\log(1+t) \geq \frac{t^2 + 2t}{2(1+t)}, \quad \text{for every } -1 < t \leq 0. \quad (\text{A.34})$$

This can be checked just observing that the function defined as the left-hand side minus the right-hand side of (A.34) is null at zero and has a non-positive derivative. We also recall the following 1-dimensional real analysis result, which will be useful as well.

Lemma 1. *Let $\mathcal{J} \subset \mathbb{R}$ be an open interval. Let $f \in C^1(\mathcal{J})$ and assume that whenever $f'(t) = 0$, for some $t \in \mathcal{J}$, the second derivative of f at t exists and is such that $f''(t) > 0$. Then the function f has at most one stationary point, which is a global minimizer.*

With the following lemma we show that $p(\theta, \cdot)$ has a unique global minimum in $[1, +\infty)$.

Lemma 2. *There exists an open interval $\mathcal{I} \ni 1$ and a unique smooth function $\varphi : \mathcal{I} \rightarrow (1, +\infty)$ such that*

$$\underset{t \in [1, +\infty)}{\operatorname{argmin}} p(\theta, t) = \varphi(\theta), \quad \text{for every } \theta \in \mathcal{I}.$$

Proof. Set $\bar{p} := p(1, \cdot)$. First, note that the derivative of \bar{p} reads as

$$\bar{p}'(t) = \frac{v\bar{N}}{t^{1/3}} + \frac{d}{dt}W_{vol}^\chi(t) - \frac{\mu}{kT} = \frac{v\bar{N}}{t^{1/3}} + \log\left(1 - \frac{1}{t}\right) + \frac{1}{t} + \frac{\chi}{t^2} - \frac{\mu}{kT}, \quad \text{for every } t > 1.$$

Let $h(t) := \log\left(\frac{t}{t-1}\right) - \frac{1}{t} - \frac{1}{2t^2}$ for every $t \in (1, +\infty)$. Note that $h(t) \geq 0$ for every $t \in (1, +\infty)$ and that $t^2h(t) \rightarrow 0$ as $t \rightarrow +\infty$. It is straightforward to check that $\lim_{t \rightarrow 1} \bar{p}'(t) = -\infty$ and $\lim_{t \rightarrow +\infty} \bar{p}'(t) = -\frac{\mu}{kT} \geq 0$. Moreover, one has that

$$\bar{p}'(t) \geq 0 \Leftrightarrow t^2\bar{p}'(t) \geq 0 \Leftrightarrow v\bar{N}t^{5/3} - (1/2 - \chi) - t^2h(t) - \frac{\mu}{kT}t^2 \geq 0.$$

Since $\lim_{t \rightarrow +\infty} v\bar{N}t^{5/3} - (1/2 - \chi) - t^2h(t) - \frac{\mu}{kT}t^2 = +\infty$, the existence of $t \in (1, +\infty)$ such that $\bar{p}'(t) = 0$ is guaranteed. The uniqueness of such $t \in (1, +\infty)$ follows from the above Lemma 1. Indeed, by using (A.34), one finds that $(t^2\bar{p}'(t))' > 0$ for every $t \in (1, +\infty)$. Since $(t^2\bar{p}'(t))' = 2t\bar{p}'(t) + t^2\bar{p}''(t)$, we get that $\bar{p}'(t) = 0$ implies $\bar{p}''(t) > 0$. Therefore, by Lemma 1, there is a unique stationary point $t_{\min} \in (1, +\infty)$, which is also the global minimizer of \bar{p} . Recall that

$$0 = \bar{p}'(t_{\min}) = p_t(1, t_{\min}) \quad \text{and} \quad 0 < \bar{p}''(t_{\min}) = p_{tt}(1, t_{\min}).$$

By applying the Implicit Function Theorem we get that there exist an open neighborhood $\mathcal{I} \subseteq (0, +\infty)$ of 1, an open neighborhood $\mathcal{J} \subseteq (1, +\infty)$ of t_1 and a unique smooth function $\varphi : \mathcal{I} \rightarrow \mathcal{J}$, such that

$$\{(\theta, \varphi(\theta)) : \theta \in \mathcal{I}\} = \{(\theta, t) \in \mathcal{I} \times \mathcal{J} : p_t(\theta, t) = 0\}.$$

At the same time, one can check, as above, that $p_t(\theta, t) = 0$ implies $p_{tt}(\theta, t) > 0$, for every $\theta \in \mathcal{I}$. Hence, again by Lemma 1, the following smooth map is well-defined

$$(0, +\infty) \ni \theta \mapsto \varphi(\theta) = \operatorname{argmin}_{[1, +\infty)} p(\theta, \cdot) \in (1, +\infty).$$

This concludes the proof of the lemma. \square

For the sake of brevity, we introduce the following notation. Let the interval $\mathbb{R} \supset \mathcal{I} \ni 1$ and the function φ be given by Lemma 2. For any $\theta \in \mathcal{I}$, set

$$\alpha_\theta := \sqrt[3]{\varphi(\theta)} > 1, \quad \text{and} \quad \alpha := \alpha_1, \quad (\text{A.35})$$

and define the function

$$W_\theta(F) := \frac{\sqrt{N}\theta}{2}(|F|^2 - 3) + W_{vol}^\chi(\det F) - \frac{\mu}{kT}(\det F - 1), \quad \text{for every } F \in \mathbb{R}_1^{3 \times 3}. \quad (\text{A.36})$$

According to this notation, for every $x \in \Omega_h$ and every h sufficiently small we have that

$$W_h(x, F) = W_{f_h(x)}(F). \quad (\text{A.37})$$

Properties of the family $\{W_h\}$ Hereafter we gather some properties satisfied by the family of 3D energy densities $\{W_h\}$ and by its approximate variant $\{\widehat{W}_h\}$ defined in (4.21).

Energy wells

Lemma 3. *Let the interval $\mathbb{R} \supset \mathcal{I} \ni 1$ and the function φ be given by Lemma 2. For every $\theta \in \mathcal{I}$, the function W_θ is minimized precisely on the set $\alpha_\theta \operatorname{SO}(3)$, with α_θ defined as in (A.35).*

Proof. Fix $\theta \in \mathcal{I}$ and denote $m_\theta := \min_{[1, +\infty)} p(\theta, \cdot) = p(\theta, \alpha_\theta^3)$. From inequality (A.32) and by definition of p , we have that $W_\theta(F) \geq p(\theta, \det F) \geq m_\theta$, for every $F \in \mathbb{R}_1^{3 \times 3}$. Suppose that $W_\theta(F) = m_\theta$, for some $F \in \mathbb{R}_1^{3 \times 3}$. By the definition of p given by (A.33), F must satisfy $|F|^2 = 3(\det F)^{2/3}$. This implies that all eigenvalues of the positive symmetric matrix $F^\top F$ are equal to some $\lambda^2 \in \mathbb{R} \setminus \{0\}$, by (A.32), and accordingly $F \in \lambda \operatorname{SO}(3)$. On the other hand, it must be $\lambda^3 = \det F = \alpha_\theta^3$ (by uniqueness of the minimizer of $p(\theta, \cdot)$), implying that indeed $F \in \alpha \operatorname{SO}(3)$.

Conversely, let $F = \alpha_\theta R$ for some $R \in \operatorname{SO}(3)$. Then $|F|^2 = 3\alpha_\theta^2 = 3(\alpha_\theta^3)^{2/3} = 3(\det F)^{2/3}$ and thus $W_\theta(F) = m_\theta$. \square

Taking into account (A.37) and the above lemma, we have that

$$W_h(x, \cdot) \quad \text{attains its minimum precisely at} \quad \alpha_{f_h(x)} \operatorname{SO}(3). \quad (\text{A.38})$$

Finally, from (A.35) and from definition (A.31) of $f_h(x)$, we have that for every $x \in \omega_i \times (-h/2, 0]$ (similarly, for $x \in \omega_i \times (0, h/2)$), $i = 1, \dots, n$,

$$\alpha_{f_h(x)} = \sqrt[3]{\varphi \left(1 - \frac{h}{h_0} \frac{M_i}{N} \right)} = \alpha - \frac{h}{h_0} \beta M_i + o(h), \quad \text{with } \beta := \frac{\varphi'(1)}{3N}, \quad (\text{A.39})$$

by Taylor expansion. This gives the energy well $U_h(x)\text{SO}(3)$ defined in (2.4)–(2.6). Let us stress the fact that a crucial property of $U_h(x)$ which allows us to use [1, Theorem 2.6] is that such spontaneous stretch field has the structure $U_h(x) = \alpha I_3 + hB(x)$, with $\int_{-h/2}^{h/2} B(x', x_3) dx_3 = 0$. Note that this fact is connected with the structure of the chosen density $N_h(x)$ of polymer chains (see (2.1) and the subsequent sentence).

Remark 1. The above analysis on the energy wells of W_h can be rephrased for the variant \widehat{W}_h introduced in Section 4, namely to

$$\widehat{W}_h(x, F) := \frac{v\bar{N}f_h(x)}{2}(|F|^2 - 1) + \frac{1-2\chi}{2\det F}. \quad (\text{A.40})$$

Indeed, defining the auxiliary function

$$\hat{p}(t, \theta) := \frac{3v\bar{N}\theta}{2}(t^{2/3} - 1) + \frac{1-2\chi}{2t},$$

for $t \in [1, +\infty)$, we have that $\widehat{W}_h(x, F) \geq \hat{p}(\det F, f_h(x))$, again thanks to inequality (A.32). Also, the very same argument as in the proof of Lemma 3 give that

$$\operatorname{argmin}_{\mathbb{R}_1^{3 \times 3}} \widehat{W}_h(x, \cdot) = \left(\operatorname{argmin}_{[1, +\infty)} \hat{p}(\cdot, f_h(x)) \right)^{\frac{1}{3}} \text{SO}(3). \quad (\text{A.41})$$

Note that in this case there is no need of the Implicit Function Theorem to determine the minimizer of $p(\cdot, f_h(x))$: a straightforward computation yields the explicit formula

$$\operatorname{argmin}_{[1, +\infty)} \hat{p}(\cdot, f_h(x)) = \left(\frac{1-2\chi}{2v\bar{N}f_h(x)} \right)^{3/5}. \quad (\text{A.42})$$

Using now definition (A.31) of $f_h(x)$ and Taylor expanding, from (A.41)–(A.42) we deduce (4.22)–(4.24). ■

Regularity The function W_θ is of class C^∞ on the set $\{F \in \mathbb{R}^{3 \times 3} : \det F > 1\}$ and is continuous on $\mathbb{R}_1^{3 \times 3}$. By direct computations, we have for all $F \in \mathbb{R}^{3 \times 3}$ with $\det F > 1$ and $M, N \in \mathbb{R}^{3 \times 3}$ that

$$DW_\theta(F)[M] = v\bar{N}\theta F \cdot M + \left(1 - \det F \log \left(\frac{\det F}{\det F - 1} \right) + \frac{\chi}{\det F} - \frac{\mu}{kT} \det F \right) F^{-\top} \cdot M, \quad (\text{A.43})$$

and

$$\begin{aligned} D^2W_\theta(F)[M, N] &= v\bar{N}\theta N \cdot M + \left(-1 + \det F \log \left(\frac{\det F}{\det F - 1} \right) - \frac{\chi}{\det F} + \frac{\mu}{kT} \det F \right) F^{-\top} N^\top F^{-\top} \cdot M \\ &\quad + \left(-\det F \log \left(\frac{\det F}{\det F - 1} \right) + \frac{\det F}{\det F - 1} - \frac{\chi}{\det F} - \frac{\mu}{kT} \det F \right) (F^{-\top} \cdot N) (F^{-\top} \cdot M). \end{aligned} \quad (\text{A.44})$$

Uniform convergence By the definition of W_θ , it is clear that for any sequence $\theta_n \rightarrow 1$ the sequence $\{W_{\theta_n}\}$ uniformly converges to $W = W_1$, as $n \rightarrow +\infty$, on any compact subset of $\{F \in \mathbb{R}^{3 \times 3} : \det F > 1\}$. Moreover, in light of (A.43) and (A.44), one can show that there exists an open neighborhood \mathcal{U} of $\alpha\text{SO}(3)$ such that

$$\|W_{\theta_n} - W\|_{C^2(\overline{\mathcal{U}})} \rightarrow 0, \quad \text{as } n \rightarrow \infty.$$

Taking into account (A.37), this convergence implies in particular the following uniform convergence:

$$\operatorname{ess\,sup}_{x \in \Omega_h} \|W_h(x, \cdot) - W\|_{C^2(\overline{\mathcal{U}})} \rightarrow 0, \quad \text{as } h \rightarrow 0. \quad (\text{A.45})$$

Remark 2. A simple and interesting observation, which relates W_h with the limiting (homogeneous) density W , is that W_h cannot be rewritten in the “prestretch” form

$$W_h(x, F) = W(\alpha F U_h^{-1}(x)),$$

where $U_h(x)$ minimizes $W_h(x, F)$ at each $x \in \Omega_h$. This is instead the case, for instance, in [2, 3, 22, 23] or [18]. ■

Quadratic growth Let \mathcal{I} be given by Lemma 2 and let $\theta \in \mathcal{I}$. By plugging $F = \alpha_\theta \mathbf{I}_3$ into the expression (A.44), we get that

$$D^2 W_\theta(\alpha_\theta \mathbf{I}_3)[M]^2 = D^2 W^\theta(\alpha_\theta \mathbf{I}_3)[M_{\text{sym}}]^2 = G_\theta |M_{\text{sym}}|^2 + \lambda(\alpha_\theta)(\text{tr} M)^2, \quad M \in \mathbb{R}^{3 \times 3}, \quad (\text{A.46})$$

$$G_\theta := 2v\bar{N}\theta > 0 \quad \text{and} \quad \lambda(\alpha_\theta) := -v\bar{N}\theta - \frac{1}{\alpha_\theta^2} + \frac{\alpha_\theta}{\alpha_\theta^3 - 1} - \frac{2\chi}{\alpha_\theta^5}. \quad (\text{A.47})$$

Note that $\lambda(\alpha_\theta) > 0$ as well. Indeed, by definition (A.35) of α_θ and by Lemma 2, we have that $p_t(\theta, \alpha_\theta^3) = 0$ (see (A.33) for the definition of p), or, equivalently, that

$$v\bar{N}\theta + \alpha_\theta \log\left(1 - \frac{1}{\alpha_\theta^3}\right) + \frac{1}{\alpha_\theta^2} + \frac{\chi}{\alpha_\theta^5} - \frac{\alpha_\theta \mu}{kT} = 0.$$

As a consequence, $\lambda(\alpha_\theta)$ can be rewritten as

$$\lambda(\alpha_\theta) = \frac{\alpha_\theta}{\alpha_\theta^3 - 1} + \alpha_\theta \log\left(1 - \frac{1}{\alpha_\theta^3}\right) - \frac{\chi}{\alpha_\theta^5} - \frac{\mu \alpha_\theta}{kT}.$$

Then (A.34) yields

$$\lambda(\alpha_\theta) \geq \frac{(1 - 2\chi)\alpha_\theta^3 + 2\chi}{2\alpha_\theta^5(\alpha_\theta^3 - 1)} - \frac{\mu \alpha_\theta}{kT} > 0, \quad (\text{A.48})$$

where the last strict inequality is due to the fact that $0 < \chi \leq 1/2$ and $\mu \leq 0$.

Now, note that all the differentials of W_θ of order greater than or equal to 3 do not depend on θ . Hence, by Taylor expansion of W_θ around $\alpha\mathbf{I}_3$ and by the positivity of G_θ and $\lambda(\alpha_\theta)$ we have that

$$W_\theta(F) \geq \tilde{C}|F^\top F - \alpha_\theta^2 \mathbf{I}_3|^2 \geq C \operatorname{dist}^2(F, \alpha_\theta \text{SO}(3)),$$

for every F in a neighborhood of $\alpha_\theta \text{SO}(3)$. This fact, together with Lemma 3 and the quadratic growth of W_θ at ∞ , shows in particular that

$$W_h(x, F) \geq C \text{dist}^2(F, \text{SO}(3)U_h(x)), \quad \text{for every } F \in \mathbb{R}_1^{3 \times 3}, \quad (\text{A.49})$$

with $U_h(x)$ given by (2.6).

The listed properties show that the family $\{W_h\}$ of 3D energy densities – up to a multiplicative factor α , which is only a matter of the appropriate change of variable (as explained below) – satisfies the hypothesis of [1, Theorem 2.6]. We can then rigorously derive the (new) corresponding 2D model (2.12).

The 2D model We recall that the 3D-to-2D model reduction of [1] which we aim to use is derived therein for 3D spontaneous stretch fields $I_3 + hB(x)$, whereas in the present setting such fields are of the form $\alpha I_3 + hB(x)$, for some $\alpha > 1$. To reduce to the setting of [1], it is sufficient to observe that, setting $\tilde{\Omega} := \alpha\omega \times (-1/2, 1/2)$,

$$\mathcal{E}_h(v) := \int_{\Omega_h} W_h(x, \nabla v(x)) dx = \frac{h}{\alpha^2} \int_{\tilde{\Omega}} W_h\left(\left(\frac{\tilde{x}'}{\alpha}, h\tilde{x}_3\right), \alpha \nabla_{ah}\tilde{v}(\tilde{x})\right) d\tilde{x}, \quad (\text{A.50})$$

where $\tilde{v} : \tilde{\Omega} \rightarrow \mathbb{R}^3$ and $\tilde{v}(\tilde{x}', \tilde{x}_3) := v(\tilde{x}'/\alpha, h\tilde{x}_3)$. Now, setting

$$\tilde{N}_h^\alpha(\tilde{x}) := \begin{cases} \bar{N} - \frac{h}{\alpha h_0} M_i, & \text{for } \tilde{x} \in \alpha\omega_i \times (-1/2, 0], \\ \bar{N} + \frac{h}{\alpha h_0} M_i, & \text{for } \tilde{x} \in \alpha\omega_i \times (0, 1/2). \end{cases}$$

and, accordingly, defining

$$\tilde{W}_h^\alpha(\tilde{x}, F) := \frac{v\tilde{N}_h^\alpha(\tilde{x})}{2} (\alpha^2 |F|^2 - 3) + W_{vol}^\chi(\alpha^3 \det F) - \frac{\mu}{kT} (\alpha^3 \det F - 1), \quad (\tilde{x}, F) \in \tilde{\Omega} \times \mathbb{R}_1^{3 \times 3},$$

we have from definition (A.30) that $W_h((\tilde{x}'/\alpha, h\tilde{x}_3), \alpha F) = \tilde{W}_{ah}^\alpha(\tilde{x}, F)$. In turn, we obtain from (A.50) that

$$\frac{\mathcal{E}_h(v)}{h^3} = \frac{1}{(ah)^2} \int_{\tilde{\Omega}} \tilde{W}_{ah}^\alpha(\tilde{x}, \nabla_{ah}\tilde{v}(\tilde{x})) d\tilde{x}.$$

We have thus reduced to compute the Γ -limit, as $\varepsilon \rightarrow 0$, of $(1/\varepsilon^2) \int_{\tilde{\Omega}} \tilde{W}_\varepsilon^\alpha(\tilde{x}, \nabla_\varepsilon \tilde{v}) d\tilde{x}$, where

$$\operatorname{argmin}_{\mathbb{R}_1^{3 \times 3}} \tilde{W}_\varepsilon^\alpha(\tilde{x}, \cdot) = \left(I_3 + \varepsilon \tilde{B}^\alpha(\tilde{x}) + o(\varepsilon) \right) \text{SO}(3),$$

with

$$\tilde{B}^\alpha(\tilde{x}) := \begin{cases} -\frac{\beta M_i}{\alpha^2 h_0} I_3, & \text{if } \tilde{x} \in \alpha\omega_i \times (-1/2, 0], \\ +\frac{\beta M_i}{\alpha^2 h_0} I_3, & \text{if } \tilde{x} \in \alpha\omega_i \times (0, 1/2). \end{cases}$$

Note also that $\tilde{W}_\varepsilon^\alpha$ converges uniformly, as $\varepsilon \rightarrow 0$, to \tilde{W}^α , where $\tilde{W}^\alpha(F) = W(\alpha F)$ and W is defined as in (A.36) with $\theta = 1$. Hence, using [1], we can compute such Γ -limit $\tilde{\mathcal{E}}_0$, which is given by

$$\tilde{\mathcal{E}}_0(\tilde{u}) = \frac{1}{24} \int_{\alpha\omega} \tilde{Q}_2^\alpha(A_{\tilde{u}}(\tilde{x}') - \tilde{A}^\alpha(\tilde{x}')) d\tilde{x}' + \text{ad.t.}, \quad \tilde{u} \in W_{1,\text{iso}}^{2,2}(\alpha\omega).$$

In this expression, the quadratic form \tilde{Q}_2^α is defined, for every $F \in \mathbb{R}^{2 \times 2}$, as

$$\begin{aligned} \tilde{Q}_2^\alpha(F) &:= \min_{b \in \mathbb{R}^2, a \in \mathbb{R}} D^2 \tilde{W}^\alpha(I_3) \left[\begin{pmatrix} F & b \\ 0 & 0 \\ 0 & a \end{pmatrix} \right]^2 \\ &= \alpha^2 \min_{b \in \mathbb{R}^2, a \in \mathbb{R}} D^2 W(\alpha I_3) \left[\begin{pmatrix} F & b \\ 0 & 0 \\ 0 & a \end{pmatrix} \right]^2 \\ &= \alpha^2 (2G_1|F|^2 + \Lambda(\alpha_1)\text{tr}^2 F) =: \alpha^2 Q_2(F), \end{aligned} \quad (\text{A.51})$$

where in the third equality the minimum problem has been solved by using the explicit expression (A.46) (with $\theta = 1$), and where $\Lambda(\alpha_1) := 2G_1\lambda(\alpha_1)/(2G_1 + \lambda(\alpha_1))$, with G_1 and $\lambda(\alpha_1)$ given by (A.47). Moreover, in the above expression for $\tilde{\mathcal{E}}_0$, we have that

$$\tilde{A}^\alpha(\tilde{x}') := 12 \int_{-1/2}^{1/2} t \tilde{B}_{2 \times 2}^\alpha(\tilde{x}', t) dt = 3 \frac{\beta M_i}{\alpha^2 h_0} I_2, \quad \text{for every } \tilde{x}' \in \alpha\omega_i,$$

and

$$\text{ad.t.} := \frac{1}{2} \int_{\alpha\omega} \int_{-1/2}^{1/2} \tilde{Q}_2^\alpha(\tilde{B}_{2 \times 2}^\alpha(\tilde{x}', t)) dt d\tilde{x}' - 6 \int_{\alpha\omega} \tilde{Q}_2^\alpha(\tilde{A}^\alpha(\tilde{x}')) d\tilde{x}'.$$

Finally, note that via the correspondence $\tilde{u}(\tilde{x}') = u(\tilde{x}'/\alpha)$ between $\tilde{u} \in W_{1,\text{iso}}^{2,2}(\alpha\omega)$ and $u \in W_{\alpha,\text{iso}}^{2,2}(\omega)$, and by using that $\bar{A}(x') = \alpha^2 \tilde{A}^\alpha(\alpha x')$ (see (2.9) for the definition of \bar{A}), we have that

$$\tilde{\mathcal{E}}_0(\tilde{u}) = \frac{1}{24} \int_\omega Q_2(A_u(x') - \bar{A}(x')) dx' + \text{ad.t..} \quad (\text{A.52})$$

By the very definition of the tensor \mathbb{C} in (2.10) it is straightforward to see that the quantity $\mathcal{E}_0(y)$ in (2.8) with the residual term (2.13) added is precisely the quantity obtained in (A.51)–(A.52).

Remark 3. We here make a couple of comments about the properties of the approximate energy densities \widehat{W}_h given in (4.21), for we will use the equivalent expression (A.40).

We start with the simple observation that the dependence on the thickness variable x_3 and the thickness parameter h in the approximate model energies \widehat{W}_h remains unchanged with respect to the original W_h . Thus, taking into account the energy well structure showed in Remark 1, it is straightforward to verify that \widehat{W}_h shares the same regularity, uniform convergence and quadratic growth properties as W_h .

In particular, the 2D model (obtained by repeating the same procedure as in the general case provided above) will be governed by the functional $\tilde{\mathcal{E}}_0$ as in (A.52), with the corresponding quadratic form Q_2 obtained via (A.51) from the second differential of the (approximate) homogeneous density \widehat{W} corresponding to \widehat{W}_h with $f_h \equiv 1$ in (A.40). Moreover, \widehat{W} is minimized at $\alpha\text{SO}(3)$ with $\alpha = (\frac{1-2\chi}{2\sqrt{N}})^{1/5}$ explicitly determined in (A.41)–(A.42). A direct computation yields

$$D^2 \widehat{W}(\alpha I_3)[F]^2 = 2v\bar{N}|F_{\text{sym}}|^2 + v\bar{N}\text{tr}^2 F, \quad F \in \mathbb{R}^{3 \times 3}$$

so that Q_2 in (A.51) equals \widehat{Q}_2 , defined as

$$\widehat{Q}_2(G) := 2v\bar{N} \left(|G_{\text{sym}}|^2 + \frac{1}{3} \text{tr}^2 G \right), \quad G \in \mathbb{R}^{2 \times 2}. \quad (\text{A.53})$$

■

Acknowledgements

This work has been funded by the European Research Council through the ERC Advanced Grant 340685-MicroMotility.

Conflict of interest

All authors declare no conflicts of interest in this paper.

References

1. Agostiniani V, Lucantonio A, Lučić D (2018) Heterogeneous elastic plates with in-plane modulation of the target curvature and applications to thin gel sheets. *ESAIM Contr Optim Ca* in press.
2. Agostiniani V, DeSimone A (2017) Rigorous derivation of active plate models for thin sheets of nematic elastomers. *Math Mech Solids* in press.
3. Agostiniani V, DeSimone A (2017) Dimension reduction via Γ -convergence for soft active materials. *Meccanica* 52: 3457–3470.
4. Klein Y, Efrati E, Sharon E (2007) Shaping of elastic sheets by prescription of non-Euclidean metrics. *Science* 315: 1116–1120.
5. Aharoni H, Sharon E, Kupferman R (2014) Geometry of thin nematic elastomer sheets. *Phys Rev Lett* 113: 257801.
6. Hamouche W, Maurini C, Vincenti A, et al. (2017) Multi-parameter actuation of a neutrally stable shell: a flexible gear-less motor. *Proc R Soc A* 473: 20170364.
7. Armon S, Efrati E, Sharon E, et al. (2011) Geometry and mechanics in the opening of chiral seed pods. *Science* 333: 1726–1730.
8. Dawson C, Vincent JFV, Rocca AM (1997) How pine cones open. *Nature* 290: 668.
9. Hu Z, Zhang X, Li Y (1995) Synthesis and application of modulated polymer gels. *Science* 269: 525–527.
10. Ionov L (2011) Soft microorigami: self-folding polymer films. *Soft Matter* 7: 6786–6791.
11. Guo W, Li M, Zhou J (2013) Modeling programmable deformation of self-folding all-polymer structures with temperature-sensitive hydrogels. *Smart Mater Struct* 22: 115028.
12. Mao Y, Yu K, Isakov MS, et al. (2015) Sequential self-folding structures by 3D printed digital shape memory polymers. *Sci Rep-UK* 5: 13616.

13. Na JH, Evans AA, Bae J, et al. (2015) Programming reversibly self-folding origami with micropatterned photo-crosslinkable polymer trilayers. *Adv Mater* 27: 79–85.
14. Liu Y, Shaw B, Dickey MD, et al. (2017) Sequential self-folding of polymer sheets. *Sci Adv* 3: e1602417.
15. Hawkes W, An B, Benbernou NM, et al. (2010) Programmable matter by folding. *P Natl Acad Sci USA* 107: 12441–12445.
16. Yoon C, Xiao R, Park J, et al. (2014) Functional stimuli responsive hydrogel devices by self-folding. *Smart Mater Struct* 23: 094008.
17. Doi M (2009) Gel dynamics. *J Phys Soc Jpn* 78: 052001.
18. Schmidt B (2007) Plate theory for stressed heterogeneous multilayers of finite bending energy. *J Math Pure Appl* 88: 107–122.
19. Lucantonio A, Nardinocchi P, Stone HA (2014) Swelling dynamics of a thin elastomeric sheet under uniaxial pre-stretch. *J Appl Phys* 115: 083505.
20. Dai HH, Song Z (2011) Some analytical formulas for the equilibrium states of a swollen hydrogel shell. *Soft Matter* 7: 8473–8483.
21. Topsøe F (2007) Some bounds for the logarithmic function, In: Cho YJ, Kim JK, Dragomir SS Editors, *Inequality theory and applications* 4, New York: Nova Science Publishers, 137.
22. DeSimone A, Teresi L (2009) Elastic energies for nematic elastomers. *Eur Phys JE* 29: 191–204.
23. DeSimone A (1999) Energetics of fine domain structures. *Ferroelectrics* 222: 275–284.



AIMS Press

© 2018 the Author(s), licensee AIMS Press. This is an open access article distributed under the terms of the Creative Commons Attribution License (<http://creativecommons.org/licenses/by/4.0>)